PNAS RESEARCH ARTICLE | ENVIRONMENTAL SCIENCES

Holocene variations in Lake Titicaca water level and their implications for sociopolitical developments in the central Andes

Stéphane Guédron[a,1], Christophe Delaere[b], Sherilyn. C. Fritz[c], Julie Tolu[d,e,f], Pierre Sabatier[g], Anne-Lise Devel[g], Carlos Heredia[h], Claire Vérin[a], Eduardo Q. Alves[i], and Paul A. Baker[j]

Edited by Cathy Whitlock, Montana State University Bozeman, Bozeman, MT; received September 16, 2022; accepted November 17, 2022

Holocene climate in the high tropical Andes was characterized by both gradual and abrupt changes, which disrupted the hydrological cycle and impacted landscapes and societies. High-resolution paleoenvironmental records are essential to contextualize archaeological data and to evaluate the sociopolitical response of ancient societies to environmental variability. Middle-to-Late Holocene water levels in Lake Titicaca were reevaluated through a transfer function model based on measurements of organic carbon stable isotopes, combined with high-resolution profiles of other geochemical variables and paleoshoreline indicators. Our reconstruction indicates that following a prolonged low stand during the Middle Holocene (4000 to 2400 BCE), lake level rose rapidly ~15 m by 1800 BCE, and then increased another 3 to 6 m in a series of steps, attaining the highest values after ~1600 CE. The largest lake-level increases coincided with major sociopolitical changes reported by archaeologists. In particular, at the end of the Formative Period (500 CE), a major lake-level rise inundated large shoreline areas and forced populations to migrate to higher elevation, likely contributing to the emergence of the Tiwanaku culture.

central Andes | Lake Titicaca sediment | biomarkers | carbon isotopes | societies

Significance

The Lake Titicaca Basin has been inhabited for millennia, and cultural development has been linked to regional climate history. We reevaluated Lake Titicaca's Holocene water-level history by integrating organic-carbon-stable-isotope measurements from multiple sediment cores with analysis of paleoshoreline indicators. We developed a lake-level model that is compatible with archaeological timescales and shows Late Holocene fluctuations of ~5 m relative to the mean values. The model suggests low stands much shorter than indicated by prior studies and a more gradual lake-level rise, consistent with reconstructions of regional precipitation. Major lake-level rises coincided with periods of cultural emergence, including the Tiwanaku culture. The general trend of increased wetness during the Late Holocene likely promoted agricultural and sociopolitical development and influenced population migration.

Lake Titicaca is a large, deep, high-elevation lake in the central Andes (Fig. 1) that is sensitive to climate variation on interannual to millennial timescales. For millennia, the lake has been an important resource for people living in the region. Many studies by different research groups over the last 50 y used diverse tools to reconstruct the history of the lake and its watershed and to infer variation in climate and its drivers. Those studies include long drill core records that span hundreds of thousands of years (1, 2) and multiple shorter records that extend from the Last Glacial Maximum (3, 4) through parts of the Holocene (5–7).

The Late Holocene (4.2 ka BP to the present) history of the Lake Titicaca Basin has been studied more intensively than have prior periods of time, in part because of its relevance to cultural development in the watershed, particularly around the southern basin of the lake, Lago Menor (also known as Lago de Huiñaymarca). During the generally arid climate of the Middle Holocene (8.2 to 4.2 ka BP), lake level in the large deep basin of Lake Titicaca, Lago Mayor, dropped as much as 85 m (9). As a consequence, most of the relatively shallow Lago Menor was desiccated (6), and there was no hydrologic connection between the northern and southern basins through the Strait of Tiquina. However, approximately 4000 y ago, lake level began to rise as the climate became wetter, Lago Mayor overflowed into Lago Menor, and the sedimentary history of the modern lacustrine phase of Lago Menor began (3).

The Lake Titicaca Basin has a rich Late Holocene archaeological record, including villages and ceremonial sites in the watershed of Lago Menor (10) and in regions of Lago Mayor proximal to the Strait of Tiquina (11). Many previous studies of these sites related changes in cultural history to lake level and climate variability, including the potential influences of this environmental variability on the initial expansion of agriculture in the Early Formative period (ca. 1500 to 800 BCE) and subsequent changes in resource use, such as pastoralism, fishing, hunting, and arable agriculture (12–14). Sociopolitical patterns, including population growth, development of powerful political and religious polities, warfare, and collapse of the Tiwanaku State also have been tied to the dynamics of the lake and climate (15–19).

Holocene lake-level variation in Lake Titicaca has been inferred from multiple types of data, including seismic profiles (9), sedimentology (5, 7), geochemistry (3, 5), diatoms (4, 20), and ostracods (21). Reconstructions based on several of these variables provided physical and quantitative constraints on lake elevation for given time intervals, including seismic and sedimentological data (7, 9, 22), as well as a transfer function based on ostracod data (21). However, the temporal resolution of these prior quantitative reconstructions is low and generally insufficient for comparison with many aspects of change in the archaeological record (10). In addition, the stratigraphic record in some of these earlier studies

Author contributions: S.G., C.D., S.C.F., and P.A.B. designed research; S.G., C.D., S.C.F., J.T., C.H., and P.A.B. performed research; S.G., J.T., P.S., A.-L.D., C.H., C.V., and E.Q.A. contributed new reagents/analytic tools; S.G., C.D., S.C.F., J.T., and P.S. analyzed data; and S.G., C.D., S.C.F., and P.A.B. wrote the paper.

The authors declare no competing interest.

This article is a PNAS Direct Submission.

[1]To whom correspondence may be addressed. Email: stephane.guedron@ird.fr.

This article contains supporting information online at https://www.pnas.org/lookup/suppl/doi:10.1073/pnas.2215882120/-/DCSupplemental.

Published January 3, 2023.

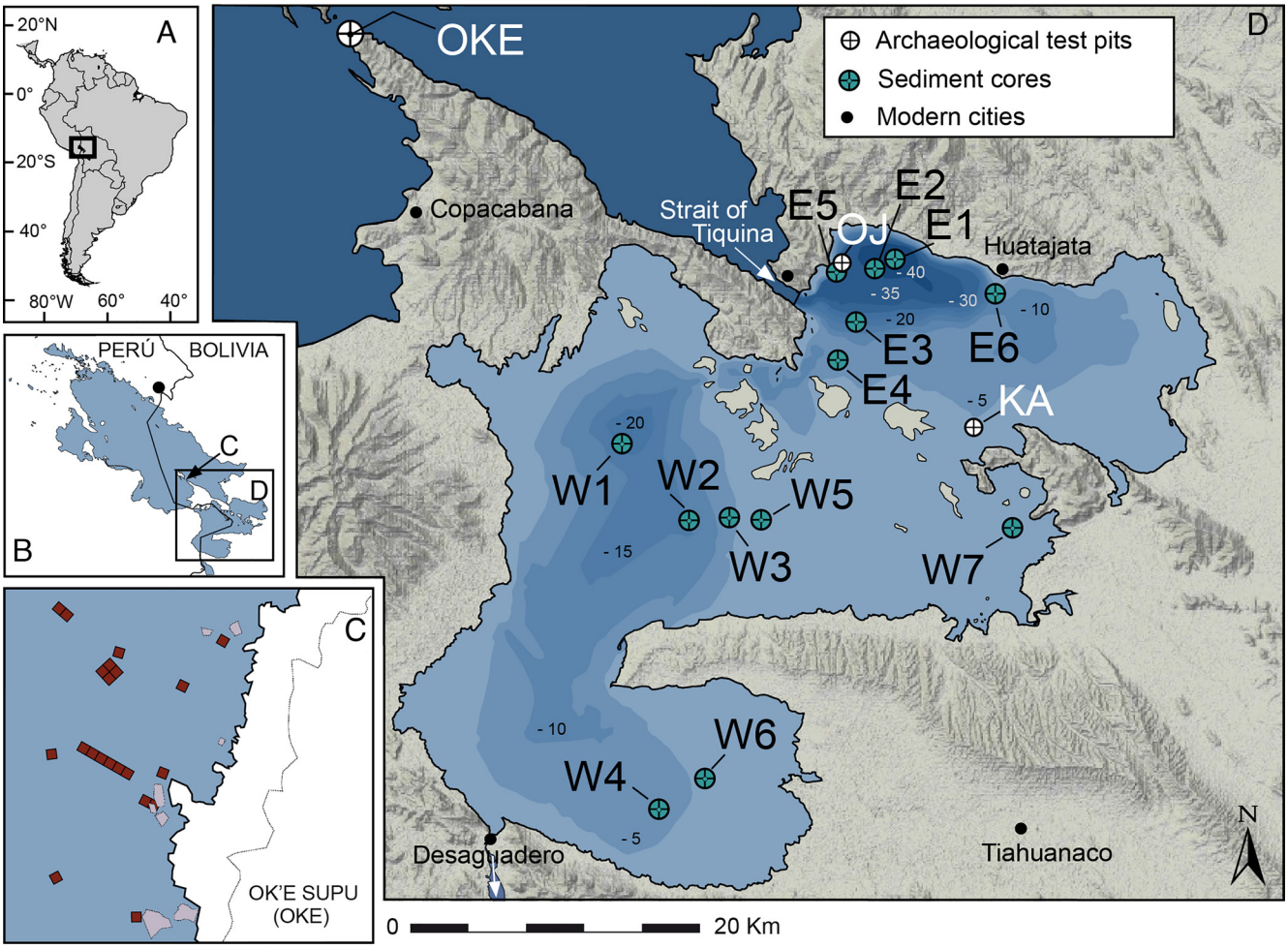

Fig. 1. (*A*) Location of Lake Titicaca in the western tropical Andes. (*B*) General map of Lake Titicaca (*C*) Ok'e Supu site (OKE) where the 18 underwater archaeological test pits (dark red squares) were excavated in Lago Mayor to the north of the Strait of Tiquina (8). (*D*) Location of the 13 sediment cores sampled in Lago Menor (W1 to W7 and E1 to E6) referenced based on their location in the eastern (E) or western (W) southern subbasin of Lake Titicaca, and of the archaeological test pits at K'anaskia (KA) and Ojelaya (OJ). All isobaths are in meters below the 3,810 masl average modern lake level.

was incomplete, because of erosional sediment loss during low-stand intervals.

Here, we present a high-resolution quantitative model of water-level variability in Lake Titicaca during the Middle to Late Holocene, inferred from a carbon isotope transfer function developed using 13 cores from the southern basin of the lake. The transfer function was calibrated using short cores whose sediments span the instrumental record of lake-level variation measured at Puno, Peru since 1915. We integrated the model reconstruction with data from 21 underwater archaeological test pits in Lago Menor and in Lago Mayor just north of the Strait of Tiquina (8), which provide sedimentological evidence of discrete intervals of past lake-level lowering. We documented changes in water chemistry (salinity) and biotic components of the aquatic ecosystem (macrophytes, algae) using multiple inorganic and organic geochemical proxies in the sediment cores to help corroborate fluctuations inferred from the transfer function. Finally, we re-evaluated sociopolitical changes inferred from the archaeological record (10) in the context of our reconstructions of water-level change in Lake Titicaca during the Late Holocene.

Settings and Transfer Function Development

Lake Titicaca (16°S, 69°W) is a high-altitude lake on the northern Altiplano (average = 3,810 masl) of Bolivia and Peru (23). The lake consists of two subbasins (Fig. 1), Lago Mayor (7,131 km^2, 125 m average depth) and Lago Menor (1,428 km^2, 9 m average depth), connected by the Strait of Tiquina (39.5 m depth, *SI Appendix*, Fig. S1). When the lake level exceeds 3,804 masl, the lake discharges southward via the Río Desaguadero into the southern Altiplano to Lago Poopo.

Lake-level fluctuations are driven by the relative balance between precipitation and riverine inflow, and evaporation (which is closely linked to temperature and solar radiation) and riverine outflow. Variations in lake level can be used to infer fluctuations in this moisture balance. A substantial portion of the moisture variation is controlled by the changing intensity of the South American Summer Monsoon (SASM). During the instrumental period (1915 to 2022), evaporation has accounted for ~90% of water output (23), the remainder being attributed to the highly variable flow of the only outlet, the Rio Desaguadero. Annual lake-level rise (driven by the SASM seasonality) and fall averages ~0.69 m. Variability of lake-level rise is greater than variability of lake-level fall, and interannual fluctuations in lake level are correlated with precipitation variability (3). Over the last century, the total range of lake-level variation was ~6 m (24).

Both sediment cores and underwater archaeological test pits (*SI Appendix*, Figs. S2 and S3) enabled the identification of intervals of past lake-level lowering, including exposure surfaces (i.e., peat beds and gleyed soil), erosion surfaces or paleoshorelines

(i.e., scour marks, abrupt transitions to dense sandy sediments, and highly fragmented shell materials), and non-depositional environments (i.e., soil horizons and hiatuses in sedimentation characterized by abrupt changes in radiocarbon ages). In addition, changes in the source of organic matter, as recorded by its carbon stable isotope signature, can be used to reconstruct historical displacements of the littoral margins (5). Along the gentle slopes of Lago Menor [average slope = 0.04 ± 0.01% (25, 26)], littoral areas <2 m deep are mainly colonized by emergent sedges (*Schoenoplectus totora*) and to a lesser extent by Hydrocharitaceae (*Elodea sp*.), Lemnaceae, and Haloragaceae (*Myriophyllum sp*.). Benthic macrophytes (e.g., *Chara*ceae and *Potamogetonaceae*) are found between 2.5 and 15 m depth, with maximum development of *Characeae* between 4.5 and 7.5 m (27). Stable isotope values of sediment organic carbon ($\delta^{13}C_{org}$) in the euphotic zone are more negative at depths less than 2.5 m, with values typical of emergent C3 sedges (av. = −25.6 ± 1.1‰), and higher at water depths between 2.5 and 15 m, with values characteristic of *Characeae* $\delta^{13}C_{org}$ (av. = −10.2 ± 0.8‰) (*SI Appendix,* Fig. S4). In the aphotic areas (>15 m deep), the sediment $\delta^{13}C_{org}$ values are dominated by those of pelagic algae (av. $\delta^{13}C_{org}$ = −23 ± 2‰). The imprint of this ecological distribution with contrasting $\delta^{13}C_{org}$ values along the slopes is inherited by the underlying sediments (5, 27–29) (*SI Appendix,* Table S1 and Fig. S4). Eroded soil organic material (av. $\delta^{13}C_{org}$ = −24.5 ± 0.9‰) can also affect the $\delta^{13}C_{org}$ values of littoral sediments through mixing processes. In deeper areas, atmospheric deposition (i.e., soil dust) during dry periods may reduce carbon isotope values (30, 31).

To reconstruct a continuous history of Middle to Late Holocene water level for Lago Menor, 13 short sediment cores were taken at water depths ranging from 3 to 43 m below the modern lake level (3,810 masl) to ensure good coverage of the amplitude of past lake-level variation (Fig. 1 and *SI Appendix,* Table S2*A*). This methodology enables different levels of resolution to be achieved as sedimentation rates and the number of sedimentary discontinuities decrease with depth. In addition, 18 underwater archaeological test pits (*SI Appendix,* Table S2*B*) were made between 1 and 15 m deep at Ok'E Supu in Lago Mayor, just north of the Strait of Tiquina (8), and 3 were dug in Lago Menor at K'anaskia and Ojelaya (*SI Appendix,* Fig. S3*E*), to refine the spatial resolution of paleoshoreline indicators and provide constraints on connectivity between the northern and southern basins of the lake. These sites were dated by determining the radiocarbon age of charcoal in selected stratigraphic layers. For each core, a transfer function (detailed below) that links the change in sediment $\delta^{13}C_{org}$ to the change in lake level was computed based on a modern maximum interannual amplitude of lake variation. Paleoshoreline data were used to constrain the lowest lake level for each time period covered by the sediment archives (*SI Appendix,* Table S3 *A* and *B*).

Based on the instrumental record of lake level over the last century (24), a depth-$\delta^{13}C_{org}$ relationship was developed and calibrated from two cores that span the last century (Fig. 2), with chronologies established from short-lived radionuclides (*SI Appendix,* Fig. S1 *A* and *B*). The model of lake-level variation for the last century (Fig. 2*A*) was based on two end-member depths, i.e., the lowest (3,807.7 masl) and highest (3,810.8 masl) average lake levels recorded in 1944 and 1986, respectively, and their associated $\delta^{13}C_{org}$ values corrected for the Suess effect (32–34). The lake level was modeled using a transfer function (TFC_{org}) following Eq. **1**:

$$\Delta\delta^{13}C_{org}/\Delta_{lake\ level} = \frac{[(-14.65) - (-16.88)]}{3810.8 - 3807.7} = 0.59‰/\text{m}. \quad [1]$$

Within the sediment cores and archaeological test pits (8), dated paleosoils and paleoshorelines were identified (*SI Appendix,* Table S3*C*), which enables us to constrain the elevation of multiple high and low stands (Fig. 2*B*). The lithologies of the cores were correlated to develop a composite stratigraphy within depth transects (*SI Appendix,* Fig. S2).

Within each lithological unit, the lowest (highest) $\delta^{13}C_{org}$ value was associated with the highest (lowest) lake-level elevation end-member (i.e., EMt and EMb, with b as the bottom and t as the top), and the lake level of each unit was modeled following Eq. **2**:

$$\text{Modeled LL} = \text{EMb} + \text{TFC}_{org} * \Delta\delta^{13}C_{org}, \quad [2]$$

where $\Delta\delta^{13}C_{org}$ is the difference between the $\delta^{13}C_{org}$ of EMb and that of the depth considered in the profile. For intervals without high-stand end-members (EM), we used the maximum value of lake-level variation from the 100-y instrumental record (24).

Models were developed for each core (Fig. 2*B*) and subsequently combined into a single curve (Fig. 3) by averaging over 25-y intervals for the period 1913 to 1750 CE, 50-y intervals for the period 1700 CE to 900 BCE, 100-y intervals from 1000 to 2400 BCE, and 500-y intervals from 4000 to 6000 BCE, with the decrease in resolution of the dataset associated with increasing age (Fig. 2). To constrain the timing and amplitude of lake-level variations, we used several complementary methods, including paleobiotic, geochemical, and sedimentological analyses, as well as information on the paleohydrology and paleoprecipitation of the central Altiplano.

The fraction of freshwater algal biomarkers (*n*-alkane $C_{25\text{-}31}$) provides information about the water depth and salinity of the lake (increasing values with rising lake level and decreasing salinity) (30). Chlorophyll was used as a proxy for algal productivity (36), which was found to reflect primarily the productivity for *Characeae* in Lake Titicaca, caused by better preservation in encrustations of calcium carbonate ($CaCO_3$) (30). Hence, high concentrations of benthic macrophyte biomarkers (chlorophyll) and $CaCO_3$ in shallow areas reflect higher production of *Characeae*. Elsewhere in the lake, higher $CaCO_3$ values reflect lower lake level and the resultant higher chemical precipitation of $CaCO_3$ with increasing salinity (30, 37). Finally, because soils are enriched in Ti compared to lake sediments (38), Ti was used as an inorganic tracer of detrital inputs to the lake. Soil erosion from the catchment is mainly recorded at water depths less than ~2.5 m, because the dense totora sedges on the lake's shore intercept more than 90% of terrestrial eroded particles (39). In deeper areas, the detrital contribution is likely dominated by aeolian inputs, deposited mainly during dry periods (40).

Results and Discussion

Our reconstruction provides continuous quantitative constraints on Titicaca water-level variation during the last 4000 y at multidecadal scale. The pattern of change in the reconstructed lake level (Fig. 2) tracks the measured water levels for the last century (R^2 = 0.70 and 0.73, $P < 0.01$), with maximum errors for modeled lake level of ± 2 m. The modeled error can be attributed to the lower resolution of the sediment records compared with the monitored lake level, coupled with cumulative errors associated with the age model.

This reevaluation of Lake Titicaca water-level variation provides higher temporal resolution than did previous reconstructions (7, 21) and is constrained with sedimentological data that enable the timing and amplitude of variation to be refined, particularly for the Middle and Late Holocene.

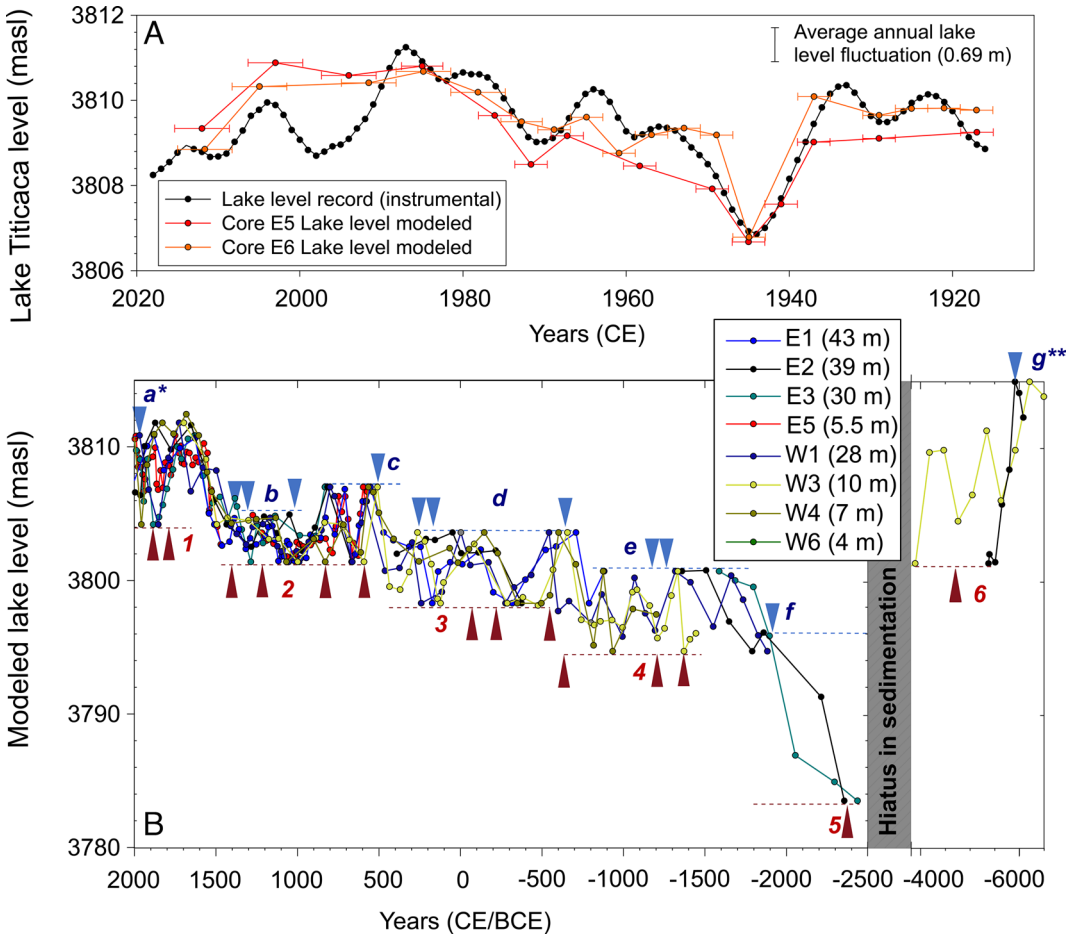

Fig. 2. Comparison of *A* the instrumental record of Lake Titicaca water-level variation over the last 100 y (24), and modeled lake levels based on the TFC_{org} of cores E5 (red symbols) and E6 (orange symbols). Horizontal error bars represent the period covered by each sediment slice in cores E5 and E6. Vertical error bar shows the average annual lake-level fluctuation (24). (*B*) Modeled lake levels based on TFC_{org} for 8 cores from the southern basin collected between 4 and 43 m below modern water depth. The period 1500 CE to modern is calibrated using the last 100 y TFC_{org}. For each period corresponding to the major stratigraphic units of the cores (*SI Appendix*, Fig. S3 *A–D* and Tables S1–S4), the elevations of the lowest and highest lake levels EM obtained using paleosoil and paleoshoreline indicators (SI Appendix, Table S3*C*) are indicated by blue (EMt) and red (EMb) triangles, respectively. The horizontal dashed lines indicate the period over which these EM are used in the model. a* is the lake level value for 1986 CE (24) and g** for 6000 BCE (3, 35).

In the Middle Holocene, from 6000 to 4000 BCE, a rapid and large-amplitude decline in lake level of ~15 m characterized the southern basin of Lake Titicaca. $\delta^{13}C_{org}$ in deep areas increased from <–22 to approximately –15‰, and *n*-alkanes $C_{25–31}$ dropped to the lowest values in the record (Fig. 3), indicating that Lake Titicaca transitioned from a deep, fresh, and overflowing lake to a shallow lake with its sediments colonized by *Characeae*. Subsequently, between 4000 and 2400 BCE, no sedimentation was evident in the cores collected in the deepest area (Chua trough), suggesting that the southern basin was almost desiccated during that interval. This observation is consistent with the conclusions of prior studies from Lago Menor (6, 21) and the Middle Holocene low stand reported for the Lago Mayor between 4000 and 3000 BCE (3, 6, 35), when lake level dropped ~85 m below the modern level (3, 9). We have reevaluated the depth of the current sill between the two basins and placed it at 39.5 m below modern lake level (*SI Appendix,* Fig. S1). Hence, during the 4000 to 2500 BCE period Lago Menor was no longer fed by Lago Mayor. This period of long-term falling lake level coincided with low austral summer insolation values and with the Northern Hemisphere (NH) Middle Holocene climate optimum. Both factors (low insolation, warm NH temperature) are known to be associated with reduced intensity of the SASM and lower amounts of precipitation (41).

Increased moisture and lake-level rise are evident in Lago Menor beginning ~2400 BCE, with the flooding of all sites located 25 m or more below modern lake level (i.e., post-hiatus lake sedimentation recovery in cores E2 and E3). Chlorophylls and $CaCO_3$ concentrations are high, and values of $\delta^{13}C_{org}$ are above –15‰ (Fig. 3), consistent with the presence of a shallow Lago Menor colonized by *Characeae*, a condition likely restricted to the deeper eastern and western troughs. These shallow conditions lasted until at least 2000 BCE, after which the lake rose rapidly during the following 500 y. Consistency between the eastern (E1, E2, and E3) and western (W1) lake-depth records suggests that both the eastern and western basins of Lago Menor were connected by a channel that passed north of Suriqui Island (*SI Appendix,* Fig. S1).

Inter-basinal flow via this connection probably occurred even when Lago Menor was below its overflow level (3,804 masl). Subsequently, all areas 10 m or more below the modern level were flooded starting around 1500 BCE (cores W2, W3), and those below 7 m were flooded around 1300 BCE (cores W4, W5), as corroborated by successive abrupt drops in Ti at these sites, which characterizes the transition between soil and overlying lake sediment (Fig. 3 and *SI Appendix,* Fig. S2). At the same time, $\delta^{13}C_{org}$, $CaCO_3$, and chlorophyll concentrations increased, indicating that sediments were flooded by more than 3 m of water, enabling *Characeae* to colonize the area.

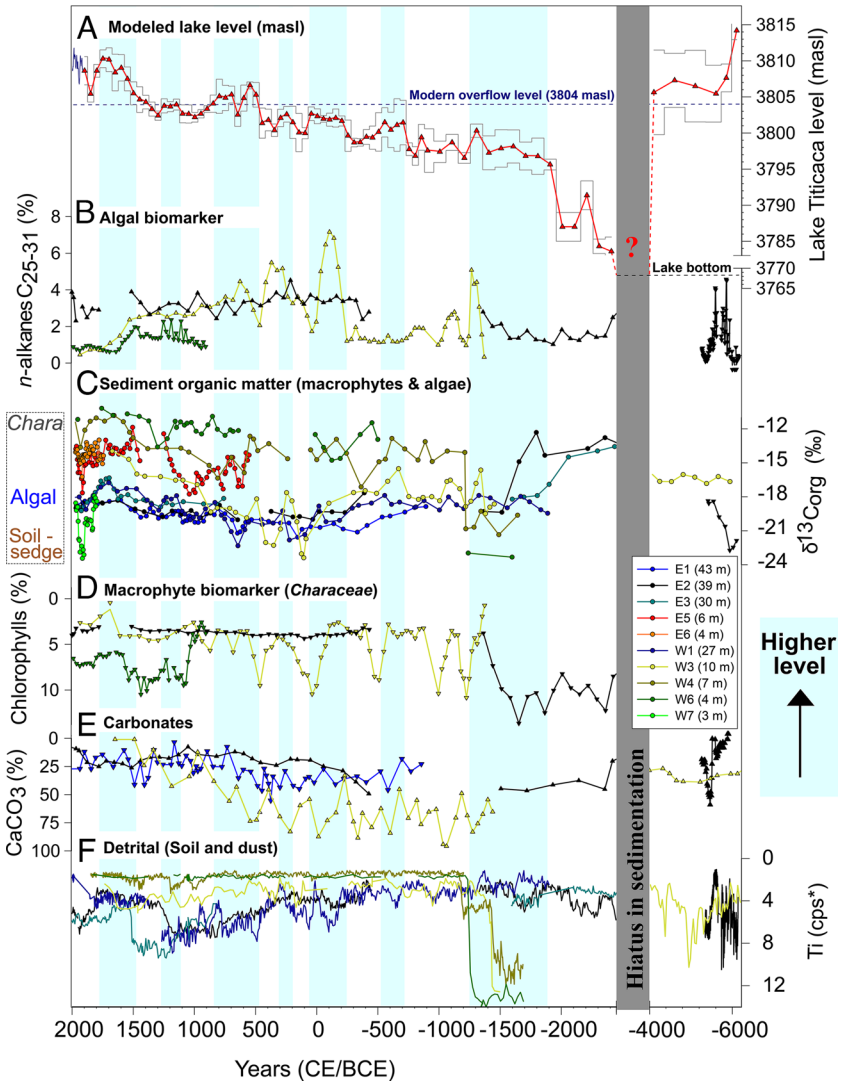

Fig. 3. (*A*) Modeled average lake level obtained from the 8 cores. The gray envelope represents the cumulative error resulting from the combination of the eight models for each time step considered. (*B*) Algal organic biomarkers (*n*-alkanes $C_{25\text{-}31}$). (*C*) Organic carbon stable isotopes ($\delta^{13}C_{org}$). (*D*) Benthic macrophyte organic biomarkers (Characeae). (*E*) Calcium carbonate ($CaCO_3$) concentration. (*F*) Titanium (Ti) abundance (*normalized independently for each core to provide a common scale). Y-axes for panels *C*–*E* are reversed. Shaded blue background lines represent intervals of high or rising lake levels from the averaged modeled lake-level curve. Cores from deep sites (>20 m) are presented in blue to black, and cores from shallow sites in green to red.

During the Late Holocene, stepwise increases in average lake level produced three phases, each with lake-level oscillations around a different baseline elevation: i) from 1300 to 700 BCE, when the lake fluctuated above and below ~3,798 masl; ii) from 700 BCE to 500 CE, with fluctuations around ~3801 masl; and iii) from 500 to 1450 CE, with fluctuations around ~3,804 masl. During that period of sequential lake-level rise, $CaCO_3$ decreased gradually, and algal biomarkers (*n*-alkanes $C_{25–31}$) increased, both in response to the progressive decrease in lake salinity associated with rising lake level (20). The reconstruction suggests that Lago Menor reached the modern overflow level after 500 CE (flooding of OJ and KA sites). In response, benthic macrophytes disappeared from the deep areas (drop in $\delta^{13}C_{org}$, $CaCO_3$, and chlorophyll) but likely colonized the newly flooded shallow ones. During the entire Late Holocene, decadal to secular lake-level declines coincided with increases in both *Characeae* biomarkers (chlorophylls and $CaCO_3$) and Ti values. For the latter proxy, one cannot exclude anthropogenic influence, because major development of agropastoralism on the lake shores occurred during the emergence of the Tiwanaku culture (42), which may have enhanced clastic inputs to the lake.

In the final period of Late Holocene lake-level increase, between 1450 and 1750 CE, lake level rose steadily to reach its modern level (>3,810 masl). The reconstructed period of lake-level rise at the beginning of the Fifteenth century is consistent with reports by Spanish chroniclers for the Inca and Colonial periods of great inundation of nearshore areas (43, 44) and corroborated by increased underwater offerings by the Inca in two ritual sites near the Island of the Sun, which were partially submersed at that time (11, 45). Following a lake level maximum at ca. 1750 CE, two substantive lake declines are reconstructed at ~1850 and 1940 CE. Both are consistent with reports of a course reversal of the Rio Désaguadero into the lake at 1835, 1845, and 1865 CE (46, 47) and the most intense recorded drought in the last century at 1943–1944 CE (21, 24).

Our reevaluation of the Middle to Late Holocene lake-level variation in Titicaca is in relatively good agreement with previous reconstructions of lake elevation from sedimentology, diatoms, and geochemistry (Fig. 4 *B*–*D*), notably for the timing of major lake rises (~1600 BCE, 700 BCE, 200 BCE, 500 CE, 800 CE, and 1500 CE) and declines (~1000 BCE, 400 BCE, 100 CE, and 1300 CE) (3, 7, 20). Our record differs in that it does not show

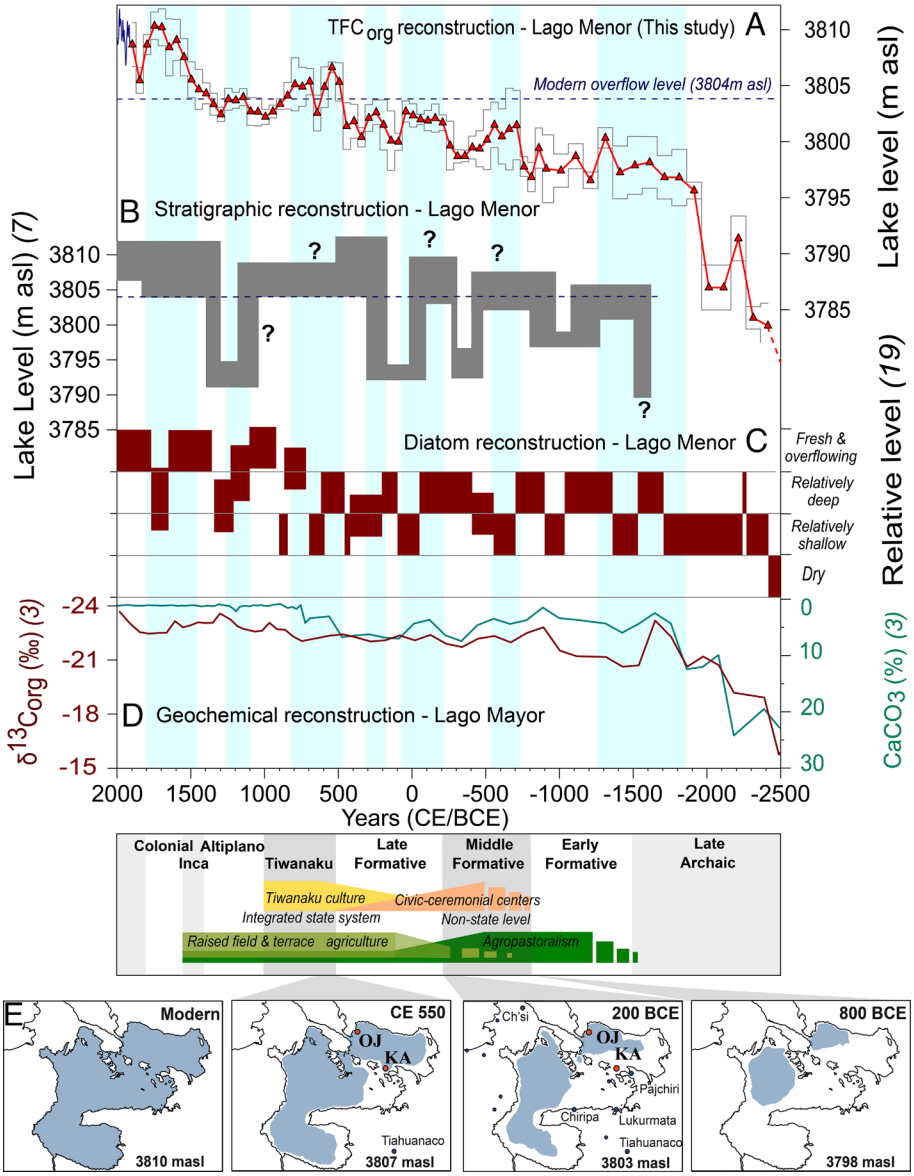

Fig. 4. (*A*) Averaged curve of Titicaca lake level (this study), (*B*) lake-level reconstruction based on sedimentological proxies (7), (*C*) lake-level reconstruction based on diatom record (20), (*D*) $\delta^{13}C_{org}$ and $CaCO_3$ profiles recorded in Lago Mayor (3), and (*E*) reconstructed lake surface of Lago Menor for an averaged paleobathymetry of 3,798 masl during the Early Formative, 3,803 masl during Middle Formative, 3,807 masl at the end of the Late Formative, and 3,810 masl for the modern period. The locations of ancient ceremonial centers in the lake area are presented as blue dots, and underwater archaeological sites currently submerged are presented as red dots. Shaded blue background lines represent intervals of high or rising lake levels from the averaged modeled lake-level curve.

abrupt changes in lake level of 10 m or more, or lowstands that persisted for centuries, such as those apparent in the stratigraphic record (7) around 300 BCE, 150 CE, and 1300 CE (Fig. 4*B*). These persistent intervals of no apparent sediment accumulation likely resulted from erosion of portions of the stratigraphic record during lowstand intervals.

The higher spatial and temporal resolution of our record relative to earlier studies yields smoother oscillations (of ~5 m) and a more gradual pattern of lake-level rise over time, which is consistent both with the observed pattern of interannual oscillations in the instrumentation period of the last century and with the evolution of regional precipitation reconstructed from the Quelccaya ice cap (48), Lake Umayo (49), Huagapo Cave (50), Huascaran ice core (51), and Lake Junin (52) (*SI Appendix*, Fig. S5).

Changes in lake stage inferred from the Middle to Late Holocene portions of our sediment record coincided with many periods of cultural change, which suggests that the inferred changes in the availability of water and arable land had consequences for people who resided around the lake. During (pre)history, the largest lake transgressions all coincided with major sociopolitical changes in the region. They include the shift from mobile hunting-gathering to a more settled agropastoral and fishing lifestyle (18) at the transition from the Late Archaic to the Early Formative period, which occurred during the 2500 to 1700 BCE abrupt lake-level rise. Persistent regional moisture during the Formative period (1500 BCE to 500 CE), which resulted in moderately high lake levels, likely promoted the expansion of agriculture, pastoralism, and the appearance of ranked societies (18, 53). In particular, the first chiefdoms and ceremonial centers, such as Tiwanaku, Chiripa, Lukurmata, and Pajchiri (Fig. 4*E*), were established around the lake during the Middle Formative period (MF: 800 to 200 BCE). At the time, all these sites were situated above the high-stand lake shoreline and therefore were protected from inundation during lake transgressions, such as those recorded at ~700 BCE and 200 BCE. Rain-fed terrace agriculture also began as early as the MF on the steep shores of Lake Titicaca

(18, 54, 55), which provided additional land to meet agricultural needs related to population growth and to compensate for the loss of land covered by the lake during the MF (Fig. 4*E*).

Early development of complex societies in the Titicaca Basin occurred primarily during the Late Formative (LF: 200 BCE to 500 CE) and involved the control of domestic labor by emergent elites, intensification of agricultural systems, development of raised field agriculture (56), expansion of interregional trade, creation of elite ideologies, and competition with other elites (18, 57). By 400 CE, Tiwanaku stood alone, and other sites, such as Lukurmata, came under its influence by ~600 CE (58). This major change in the political landscape coincided with the largest recorded lake-level rise ~500 CE (Fig. 4*A*), when the lake reached a level close to that of the present. It is likely that a large number of agricultural and potentially residential areas around ceremonial centers located in the lake basin (e.g., Lukurmata) were impacted by this transgression, with the exception of the Tiwanaku capital (Tiahuanaco), which is located farther inland. Such a transgression could also have shifted the trade routes of the llama caravan to the Yungas along the western shores of Lake Titicaca through Tiahuanaco (59). The coincident major increase in population (60–62), together with the restructuring of Tiahuanaco and the development of the agropastoral landscape, including raised field systems (13, 18, 42, 63), suggests that this event influenced a migration of human populations, from previously occupied flooded regions, to cities located on higher ground. This densification may have contributed to the rise of the Tiwanaku state. The second half of the Tiwanaku state period was drier overall, marked by a gradual decline in lake level from 850 to 1000 CE, followed by a lake level rise around 1150 CE. This latter event coincides with the terminal portions of the sedimentary hiatuses identified in previous lake-level reconstructions (7, 15) and corroborates the hypothesis that portions of those stratigraphic sequences were lost via erosion and thus the duration of dry periods was shorter than those prior reconstructions suggested. Nonetheless, although reduced precipitation during that period likely affected Tiwanaku's residents, it does not imply a drought-induced collapse of the Tiwanaku culture (15, 64), given the evidence that prolonged aridity can be endured without major cultural changes (10, 65, 66).

In general, the trend of increased wetness during the Late Holocene promoted agricultural and social development, although at times, major lake rises may have influenced population migration, because of flooding of nearshore areas. This was certainly the trigger for the emergence of the Tiwanaku culture at the expense of other early sociopolitical formations, whose arable lands were flooded during the 500 CE lake transgression. Other geoarchaeological evidence buried in the sediment of Lake Titicaca will allow us to complete and deepen the chronology and context of this pivotal period in the development of Andean societies.

Materials and Methods

Sediment Core Collection and Underwater Archaeological Prospections. Thirteen gravity cores (*SI Appendix,* Table S2*A*) were collected in Lake Titicaca between 2014 and 2017 using a Uwitec gravity corer with hammer. Detailed information for core sampling and processing is provided elsewhere (27, 67). Eighteen underwater archaeological test pits were excavated and sampled during two field campaigns in 2016 and 2018 in Lago Mayor north of the Strait of Tiquina (*SI Appendix,* Table S2*B*). Their stratigraphy and analysis of archaeological artifacts are provided elsewhere (8). Three other underwater archaeological test pits were excavated and sampled in 2017 and 2018 in Lago Menor at K'anaskia (KA) and Ojelaya (OJ) (*SI Appendix,* Table S3*E*). All information about sediment facies, unconformities, and lake level EM are provided in *SI Appendix,* Table S3*A* for the sediment cores and *SI Appendix,* Table S3*B* for the archaeological test pits.

Chronological Framework. Chronological frameworks were established with short-lived radionuclides ($^{210}Pb_{ex}$ and ^{137}Cs), analyzed using well-type germanium detectors at the Laboratoire Souterrain de Modane (LSM) following published procedures (68), and radiocarbon ages obtained from aquatic gastropods and charcoal (*SI Appendix,* Table S4), using Accelerator Mass Spectrometry (AMS) at Woods Hole Oceanographic Institution's National Ocean Sciences AMS facility, at the radiocarbon facility of the Belgian Royal Institute for Cultural Heritage (RICH), and at the Laboratoire des Sciences du Climat et de l'Environnement (LSCE/IPSL). Radiocarbon ages were calibrated to calendar years Before Present (cal. yr BP) using the calibration curve for the Southern Hemisphere SHCal20 (69) and a post-bomb curve (70) and a reservoir offset of 250 ^{14}C-yr for Lago Menor (7). The age models for cores NE98-10BXA and NE9810BXA (3) used in Fig. 4*C* were reprocessed following the same procedure. Age-depth models were generated using the Constant Flux Constant Sedimentation model using the *serac* R package (71) for uppermost core strata dated with short-lived radionuclides (E5 and E6), combined into a general model established with the *clam* R package (72). All age models are presented in *SI Appendix,* Fig. S1 *A* and *C*.

Chemical Analyses. Freeze-dried and crushed sediment and aquatic plant samples were used for all chemical analyses. Sediment dry bulk density (DBD) was obtained from the mass of a fixed freeze-dried volume of wet sediment. Total carbon content (TC, %), organic carbon content (C_{org}, %), and isotopic composition ($\delta^{13}C$ and $\delta^{13}C_{org}$, ‰) were measured by Cavity Ring-Down Spectrometer (Picarro, Inc.®) coupled with a Combustion Module (CM-CRDS, Costech, Inc.®) using previously reported analytical methods (including sample decarbonation), calibration, and sample preparation (73–76). $CaCO_3$ content was calculated from the difference between TC and C_{org} reported as molar masses. Samples for major element analysis (Ca and Ti) were digested with 10 mL of a mixture of pure acids ($HF/HCl/HNO_3$, 1:6:2), sonicated for 2 h, and heated on a hot block (120 °C, 4 h) following a published procedure (30, 77). Major elements were analyzed with an inductively coupled plasma optical spectrometer (ICP-OES, Varian 720-ES) within the analytical chemistry platform of ISTerre (OSUG-France). In all cores, analyses of titanium (Ti) were performed on the fresh surfaces of the split sediment cores every 1 to 5 mm using a nondestructive Avaatech XRF core-scanner at tube settings of 10 kV and 2 mA (78). The measured power spectra were then deconvolved into elemental relative abundances expressed in counts per second. The intensity signals of Ti abundance in Fig. 3 were normalized independently for each core to provide a common scale. Organic biomarkers were determined using pyrolysis-gas chromatography/mass spectrometry (Py-GC/MS) following the method of Tolu et al. (79) adapted for Lake Titicaca sediment (30). Briefly, the sediment samples were pyrolyzed in a Frontier Labs PY-2020iD oven (450 °C) connected to an Agilent 7890A-5975C GC–MS system. A data processing pipeline was used under the "R" computational environment to automatically detect and integrate the peaks and extract their corresponding mass spectra using the software "NIST MS Search 2" containing the library "NIST/EPA/NIH 2011" and additional spectra from published studies (79). All sediment core depth profiles for $CaCO_3$, Ti, C_{org}, and $\delta^{13}C_{org}$ are presented in *SI Appendix,* Fig. S1 *A–C*.

Data, Materials, and Software Availability. All complementary information from this study and other studies are included in the article and/or *SI Appendix*. Lake Titicaca water-level reconstruction data are archived at the Mendeley Digital commons Data repository, doi: 10.17632/9fkdt5j35v.1 (80).

ACKNOWLEDGMENTS. This work is a contribution to the PaleoBol project, supported by a grant from IRD (BQR@ISTerre2016), and TRACISOMER supported by a grant from Labex OSUG@2020 (PI: S.G.: stephane.guedron@ird.fr). S.G. (ISTerre/IRD/UGA) is part of Labex OSUG@2020 (Investissements d'avenir ANR10 LABX56). S.C.F. and P.A.B. were supported by grants from NSF (EAR-1338694, EAR-1812857, and EAR-1812681) and the National Geographic Society (9299-13). The authors thank the LSM facilities for the gamma spectrometry measurements, the EDYTEM for the X-ray fluorescence analyses, and the LSM for the gamma spectrometry facilities. Some of the ^{14}C analyses were acquired thanks to the CNRS-INSU ARTEMIS national radiocarbon AMS measurement program at Laboratoire de Mesure ^{14}C (LMC14) in the CEA Institute at Saclay (French Atomic Energy Commission). We thank M.-A. Vella, E. Brisset, K. Escobar-Torres, and C. Giguet-Covex for their help in

fieldwork; Delphine Tisserand, Sarah Bureau, and Sylvain Campillo for their help in chemical analysis (ICP-AES analysis performed within the analytical chemistry platform of ISTerre, OSUG-France); R. Bindler and the Umeå Plant Science Center for the Py-GC/MS analysis; and A. Chevalier for his help and support in radiocarbon dating at the Belgian Royal Institute for Cultural Heritage. We also wish to thank J. Gardon, A. Terrazas, C. Gonzalez, N. Clavijo, L. Salvatierra, R. Rios, J.C. Salinas, A. Castillo, M. Claure (IRD Bolivia), D. Acha (UMSA Bolivia), G. Mollericon, and la Familia Catari (Don Ramon, Don Maximo, Don Eric, Don Ruben, and Donia Maria) for their help and assistance during the field campaigns.

Author affiliations: [a]Université Grenoble Alpes, Institut des Sciences de la Terre, Institut de Recherche pour le Développement, Grenoble 38000, France; [b]Centre de Recherches en Archéologie et Patrimoine, Université libre de Bruxelles, Brussels, 1050, Belgium; [c]Department of Earth and Atmospheric Sciences and School of Biological Sciences, University of Nebraska – Lincoln, Lincoln, NE 68588; [d]Eawag, Swiss Federal Institute of Aquatic Science and Technology, Dübendorf, CH-8600, Switzerland; [e]ETH Zürich, Zürich, CH-8092, Switzerland; [f]Department of Ecology and Environmental Science, Umeå University, 901 87 Sweden; [g]Univ. Savoie Mont Blanc, Centre National de la Recherche Scientifiquel, Environnements Dynamiques et Territoires de la Montagne, Chambéry, 73000, France; [h]Laboratorio de Hidroquímica – Instituto de Investigaciones Químicas – Universidad Mayor de San Andres, Campus Universitario de Cota Cota, La Paz, casilla 3161, Bolivia; [i]Royal Belgian Institute of Natural Sciences, Bruxelles, 1000, Belgium; and [j]Division of Earth and Climate Sciences, Duke University, Durham, NC 27708

1. S. C. Fritz *et al.*, Quaternary glaciation and hydrologic variation in the South American tropics as reconstructed from the Lake Titicaca drilling project. *Quatern. Res.* **68**, 410–420 (2007).
2. A. P. Ballantyne, P. Baker, S. Fritz, B. Poulter, Climate-mediated nitrogen and carbon dynamics in a tropical watershed. *J. Geophys. Res. Biogeosci.* **116,** 11 (2011).
3. P. A. Baker *et al.*, The history of South American tropical precipitation for the past 25,000 years. *Science* **291**, 640–643 (2001).
4. P. M. Tapia, S. C. Fritz, P. A. Baker, G. O. Seltzer, R. B. Dunbar, A Late Quaternary diatom record of tropical climatic history from Lake Titicaca (Peru and Bolivia). *Palaeogeogr. Palaeoclimatol. Palaeoecol.* **194**, 139–164 (2003).
5. S. L. Cross, P. A. Baker, G. O. Seltzer, S. C. Fritz, R. B. Dunbar, A new estimate of the Holocene lowstand level of Lake Titicaca, central Andes, and implications for tropical palaeohydrology. *The Holocene* **10**, 21–32 (2000).
6. D. Wirrmann, L. F. D. O. Almeida, Low Holocene level (7700 to 3650 years ago) of Lake Titicaca (Bolivia). *Palaeogeogr. Palaeoclimatol. Palaeoecol.* **59**, 315–323 (1987).
7. M. B. Abbott, M. W. Binford, M. Brenner, K. R. Kelts, A 3500 14C yr high-resolution record of water-level changes in lake titicaca, Bolivia/Peru. *Quatern. Res.* **47**, 169–180 (1997).
8. C. Delaere, S. Guédron, The altitude of the depths: Use of inland water archaeology for the reconstruction of inundated cultural landscapes in Lake Titicaca. *Wld. Archaeol.* **54**, 67–83 (2022).
9. G. O. Seltzer, P. Baker, S. Cross, R. Dunbar, S. Fritz, High-resolution seismic reflection profiles from Lake Titicaca, Peru-Bolivia: Evidence for Holocene aridity in the tropical Andes. *Geology* **26**, 167–170 (1998).
10. M. C. Bruno *et al.*, The rise and fall of Wiñaymarka: Rethinking cultural and environmental interactions in the Southern Basin of Lake Titicaca. *Hum. Ecol.* **49**, 131–145 (2021).
11. C. Delaere, J. M. Capriles, C. Stanish, Underwater ritual offerings in the Island of the Sun and the formation of the Tiwanaku state. *Proc. Natl. Acad. Sci. U.S.A.* **116**, 8233–8238 (2019).
12. A. L. Kolata, C. Ortloff, "Tiwanaku raised-field agriculture in the Lake Titicaca Basin of Bolivia" in *Tiwanaku and Its Hinterland: Archaeology and Paleoecology of an Andean Civilization*, A. L. Kolata, Ed. (Smithsonian Institution Press, Washington, DC, 1996), **vol. 1**, pp. 109–152.
13. M. C. Bruno, Beyond raised fields: Exploring farming practices and processes of agricultural change in the ancient Lake Titicaca Basin of the Andes. *Amer. Anthrop.* **116**, 130–145 (2014).
14. J. M. Capriles, Mobile communities and pastoralist landscapes during the formative period in the Central Altiplano of Bolivia. *Latin. Amer. Antiq.* **25**, 3–26 (2014).
15. M. W. Binford *et al.*, Climate variation and the rise and fall of an Andean civilization. *Quatern. Res.* **47**, 235–248 (1997).
16. A. L. Kolata, M. W. Binford, M. Brenner, J. W. Janusek, C. Ortloff, Environmental thresholds and the empirical reality of state collapse: A response to Erickson (1999). *Antiquity* **74**, 424–426 (2000).
17. C. A. Hastorf, Community with the ancestors: Ceremonies and social memory in the Middle Formative at Chiripa, Bolivia. *J. Anthrop. Archaeol.* **22**, 305–332 (2003).
18. C. Stanish, *Ancient Titicaca: The Evolution of Complex Society in Southern Peru and Northern Bolivia* (University of California Press, 2003).
19. E. Arkush, War, chronology, and causality in the Titicaca Basin. *Latin. Amer. Antiq.* **19**, 339–373 (2008).
20. D. M. Weide *et al.*, A~ 6000 yr diatom record of mid-to late Holocene fluctuations in the level of Lago Winaymarca, Lake Titicaca (Peru/Bolivia). *Quatern. Res.* **88**, 179–192 (2017).
21. P. Mourguiart *et al.*, Holocene palaeohydrology of Lake Titicaca estimated from an ostracod-based transfer function. *Palaeogeogr. Palaeoclimatol. Palaeoecol.* **143**, 51–72 (1998).
22. S. L. Cross, P. A. Baker, G. O. Seltzer, S. C. Fritz, R. B. Dunbar, Late Quaternary climate and hydrology of tropical South America inferred from an isotopic and chemical model of Lake Titicaca, Bolivia and Peru. *Quatern. Res.* **56**, 1–9 (2001).
23. C. Dejoux, *Lake Titicaca: A Synthesis of Limnological Knowledge*, A. Iltis, Ed. (Kluwer Academic, Dordrecht (NLD), ed. IRD, 1992), **vol. 68**, p. 579.
24. J. Ronchail, J. C. Espinosa, D. Labat, J. Callede, W. Lavado, "Evolution of the Titicaca Lake level during the 20th century" in *Línea base de conocimientos sobre los recursos hidrológicos e hidrobiológicos en el sistema TDPS con enfoque en la cuenca del Lago Titicaca*, M. Aguirre, M. Pouilly, X. Lazzaro, D. Point, Eds. (UICN-IRD, La Paz, Bolivia, 2014), pp. 1–13.
25. D. Wirrmann, "Morphology and bathymetry" in *Lake Titicaca–A synthesis of limnological Knowledge*, C. Dejoux, A. Iltis, Eds. (Kluwer Academic, Dordrecht, 1992), **vol. 68**, chap. II Geomorphology and sedimentation, pp. 16–22.
26. B. Boulange, E. Aquize Jaen, Morphologie, hydrographie et climatologie du lac Titicaca et de son bassin versant. *Rev. Hydrobiol. Trop.* **14**, 269–287 (1981).
27. S. Guédron *et al.*, Diagenetic production, accumulation and sediment-water exchanges of methylmercury in contrasted sediment facies of Lake Titicaca (Bolivia). *Sci. Total Environ.* **723**, 138088 (2020).
28. M. Miller, J. Capriles, C. Hastorf, The fish of Lake Titicaca: Implications for archaeology and changing ecology through stable isotope analysis. *J. Archaeol. Sci.* **37**, 317–327 (2010).
29. H. D. Rowe *et al.*, Insolation, moisture balance and climate change on the South American Altiplano since the Last Glacial Maximum. *Clim. Change* **52**, 175–199 (2002).
30. S. Guédron *et al.*, Reconstructing two millennia of copper and silver metallurgy in the Lake Titicaca region (Bolivia/Peru) using trace metals and lead isotopic composition. *Anthropocene* **34**, 100288 (2021).
31. A. Eichler *et al.*, Ice-core evidence of earliest extensive copper metallurgy in the Andes 2700 years ago. *Sci. Rep.* **7**, 41855 (2017).
32. J. Dombrosky, A ~1000-year 13C Suess correction model for the study of past ecosystems. *The Holocene* **30**, 474–478 (2020).
33. C. D. Keeling, The Suess effect: 13Carbon-14Carbon interrelations. *Environ. Int.* **2**, 229–300 (1979).
34. H. E. Suess, "Natural radiocarbon and the rate of exchange of carbon dioxide between the atmosphere and the sea" in *Nuclear processes in geologic settings*, N. R. Council, Ed. (University of Chicago Press, Washington, DC, 1953), **vol. 43**, pp. 52–56.
35. M. Servant, S. Servant-Vildary, Holocene precipitation and atmospheric changes inferred from river paleowetlands in the Bolivian Andes. *Palaeogeogr. Palaeoclimatol. Palaeoecol.* **194**, 187–206 (2003).
36. J. Rydberg, C. A. Cook, J. Tolu, A. P. Wolfe, R. D. Vinebrooke, An assessment of chlorophyll preservation in lake sediments using multiple analytical techniques applied to the annually laminated lake sediments of Nylandssjön. *J. Paleolimnol.* **64**, 379–388 (2020).
37. K. Apolinarska, M. Pelechaty, A. Pukacz, Sedimentation by modern charophytes (Characeae): Can calcified remains and carbonate δ13C and δ18O record the ecological state of lakes–A review. *Studia Limnologica et Telmatologica* **5**, 55–65 (2011).
38. M. Jiskra *et al.*, Climatic controls on a holocene mercury stable isotope sediment record of Lake Titicaca. *ACS Earth Space Chem.* **6**, 346–357 (2022).
39. M. Pourchet *et al.*, Sédimentation récente dans le lac Titicaca (Bolivie). *C. R. Acad. Sci. Paris* **319**, 535–541 (1994).
40. A. Eichler, G. Gramlich, T. Kellerhals, L. Tobler, M. Schwikowski, Pb pollution from leaded gasoline in South America in the context of a 2000-year metallurgical history. *Sci. Adv.* **1**, e1400196 (2016).
41. P. A. Baker, S. C. Fritz, Nature and causes of Quaternary climate variation of tropical South America. *Quat. Sci. Rev.* **124**, 31–47 (2015).
42. J. W. Janusek, A. L. Kolata, Top-down or bottom-up: Rural settlement and raised field agriculture in the Lake Titicaca Basin, Bolivia. *J. Anthrop. Archaeol.* **23**, 404–430 (2004).
43. A. Ramos, *Historia de Copacabana y de su milagrosa imajen de la virjen*, R. Sans, Ed. (La Paz: Imprenta de la Unión Católica, La Paz, 1860), [1621].
44. A. F. A. Bandelier, *The Islands of Titicaca and Koati* (The Hispanic Society of America, New York, 1910), p. 716.
45. C. Delaere, J. M. Capriles, The context and meaning of an intact Inca underwater offering from Lake Titicaca. *Antiquity* **94**, 1030–1041 (2020).
46. R. Mello, La navegación en el Titicaca. *Boletín de la Sociedad Geográfica de Lima* **30**, 115–142 (1914).
47. J.-A. Vellard, *Dieux et parias des Andes: Les Ourous, ceux qui ne veulent pas être des hommes*, É. Paul, Ed. (Paul, Émile, Paris, 1954). **vol. 1**.
48. L. G. Thompson *et al.*, Annually resolved ice core records of tropical climate variability over the past~ 1800 years. *Science* **340**, 945–950 (2013).
49. P. A. Baker, S. C. Fritz, S. J. Burns, E. Ekdahl, C. A. Rigsby, "The nature and origin of decadal to millennial scale climate variability in the southern tropics of South America: The Holocene record of Lago Umayo, Peru" in *Past Climate Variability in South America and Surrounding Regions* (Springer, 2009), pp. 301–322.
50. L. C. Kanner, S. J. Burns, H. Cheng, R. L. Edwards, M. Vuille, High-resolution variability of the South American summer monsoon over the last seven millennia: Insights from a speleothem record from the central Peruvian Andes. *Quat. Sci. Rev.* **75**, 1–10 (2013).
51. L. G. Thompson, E. Mosley-Thompson, K. A. Henderson, Ice-core palaeoclimate records in tropical South America since the Last Glacial Maximum. *J. Quat. Sci.* **15**, 377–394 (2000).
52. G. Seltzer, D. Rodbell, S. Burns, Isotopic evidence for late Quaternary climatic change in tropical South America. *Geology* **28**, 35–38 (2000).
53. M. J. Miller *et al.*, Quinoa, potatoes, and llamas fueled emergent social complexity in the Lake Titicaca Basin of the Andes. *Proc. Natl. Acad. Sci. U.S.A.* **118**, e2113395118 (2021).
54. A. M. Plourde, C. Stanish, "The emergence of complex society in the Titicaca Basin: The view from the North" in *Andean Archaeology III*, (Springer, Boston, MA, 2006), chap. 9, pp. 237–257.
55. C. L. Erickson, "The dating of raised-field agriculture in the Lake Titicaca Basin, Peru" in *Pre-hispanic agricultural fields in the Andean region*, W. M. Denevan, K. Mathewson, G. Knapp, Eds. British Archaeological Reports, International Series (Oxford, 1987), **vol. 359**, pp. 373–384.
56. C. A. Hastorf, "The upper (middle and late) Formative in the Titicaca region" in *Advances in Titicaca Basin Archaeology*, C. Stanish, A. B. Cohen, M. Aldenderfer, Eds. Andean Archaeology (Cotsen Institute of Archaeology, UCLA, 2005), **vol. 1**, chap. 5, pp. 65–94.
57. C. Stanish, Formación estatal temprana en la Cuenca del Lago Titicaca, Andes surcentrales. *Bol. Arqueol. PUCP* **5**, 189–215 (2001).
58. J. W. Janusek, Craft and local power: Embedded specialization in Tiwanaku cities. *Latin. Amer. Antiq.* **10**, 107–131 (1999).
59. M. S. Bandy, Trade and social power in the southern Titicaca Basin formative. *Archeol. Pap. Am. Anthropolog. Ass.* **14**, 91–111 (2004).
60. P. S. Goldstein "Tiwanaku and Wari state expansion: Demographic and outpost colonization compared" in *Visions of Tiwanaku*, A. Vranich, C. Stanish, Eds. Cotsen Institute of Archaeology Press Monographs (Cotsen Institute of Archaeology, UCLA, 2013), **vol. 78**, pp. 41–63.
61. M. Bandy, "Tiwanaku origins and the early development: The political and moral economy of a hospitality state" in *Visions of Tiwanaku*, A. Vranich, C. Stanish, Eds. (UCLA, 2013), chap. 8, pp. 135–150.
62. M. S. Bandy, A. Vranich, A. Levine, Demographic dimensions of Tiwanaku urbanism in *Advances in Titicaca basin archaeology*, A. Vranich, A. R. Levine, Eds. Cotsen Institute of Archaeology Press Monographs (Costen Institute of Archaeology, UCLA, 2013), **vol. 2**, chap. 7, pp. 79–87.
63. M. S. Bandy, Energetic efficiency and political expediency in Titicaca Basin raised field agriculture. *J. Anthrop. Archaeol.* **24**, 271–296 (2005).

64. C. R. Ortloff, A. L. Kolata, Climate and collapse: Agro-ecological perspectives on the decline of the Tiwanaku state. *J. Archaeol. Sci.* **20**, 195–221 (1993).
65. C. L. Erickson, Neo-environmental determinism and agrarian "collapse" in Andean prehistory. *Antiquity* **73**, 634–642 (1999).
66. E. J. Marsh, Drought and the collapse of the Tiwanaku Civilization: New evidence from Lake Orurillo, Peru. *Quat. Sci. Rev.* **251**, 107004 (2021).
67. S. Guédron *et al.*, Mercury contamination level and speciation inventory in the hydrosystem of Lake Titicaca: Current status and future trends. *Environ. Pollut.* **231**, 262–270 (2017).
68. J. L. Reyss, S. Schimdt, F. Legeleux, P. Bonte, Large low background well type detectors for measurements of environmental radioactivity. *Nucl. Instrum. Methods Phys. Res. B* **357**, 391–397 (1995).
69. A. G. Hogg *et al.*, SHCal20 Southern Hemisphere Calibration, 0–55,000 Years cal BP. *Radiocarbon* **62**, 759–778 (2020).
70. Q. Hua, M. Barbetti, A. Z. Rakowski, Atmospheric radiocarbon for the period 1950–2010. *Radiocarbon* **55**, 2059–2072 (2013).
71. R. Bruel, P. Sabatier, Serac: A R package for shortlived radionuclide chronology of recent sediment cores. *J. Environ. Radioact.* **225**, 106449 (2020).
72. M. Blaauw, Methods and code for "classical" age-modelling of radiocarbon sequences. *Quat. Geochronol.* **5**, 512–518 (2010).
73. D. Balslev-Clausen, T. W. Dahl, N. Saad, M. T. Rosing, Precise and accurate $\delta^{13}C$ analysis of rock samples using flash combustion-cavity ring down laser spectroscopy. *J. Anal. At. Spectrom.* **28**, 516–523 (2013).
74. S. Guédron *et al.*, Late Holocene volcanic and anthropogenic mercury deposition in the western Central Andes (Lake Chungará, Chile). *Sci. Total Environ.* **662**, 903–914 (2019).
75. D. Paul, G. Skrzypek, I. n. Forizs, Normalization of measured stable isotopic compositions to isotope reference scales–A review. *Rapid Commun. Mass Spectrom.* **21**, 3006–3014 (2007).
76. D. Cossa *et al.*, Mercury accumulation in the sediment of the Western Mediterranean abyssal plain: A reliable archive of the late Holocene. *Geochim. Cosmochim. Acta* **309**, 1–15 (2021).
77. S. Guédron, C. Grimaldi, C. Chauvel, C. Spadini, M. Grimaldi, Weathering versus atmospheric contributions to mercury concentrations in French Guiana soils. *Appl. Geochem.* **21**, 2010–2022 (2006).
78. T. O. Richter *et al.*, "The Avaatech XRF Core Scanner: Technical description and applications to NE Atlantic sediments" in *New Techniques in Sediment Core Analysis*, R. G. Rothwell, Ed. (Geological Society, London, 2006), pp. 39–50.
79. J. Tolu, L. Gerber, J.-F. o. Boily, R. Bindler, High-throughput characterization of sediment organic matter by pyrolysis gas chromatography/mass spectrometry and multivariate curve resolution: A promising analytical tool in (paleo) limnology. *Anal. Chim. Acta* **880**, 93–102 (2015).
80. S. Guédron, Lake Titicaca Holocene water level reconstruction database. (2022) 10.17632/9fkdt5j35v. Deposited 12 November 2022.